



ELSEVIER

Available online at www.sciencedirect.com

SCIENCE @ DIRECT®

Journal of Sound and Vibration 289 (2006) 851–870

JOURNAL OF
SOUND AND
VIBRATION

www.elsevier.com/locate/jsvi

Acoustic response behaviour of panels mounted with equipment and its prediction using statistical energy analysis

K. Renji^{a,*}, P.S. Nair^a, S. Narayanan^b

^a*Structures Group, ISRO Satellite Centre, Bangalore 560017, India*

^b*Department of Applied Mechanics, Indian Institute of Technology, Madras, Chennai 600 036, India*

Received 3 December 2003; received in revised form 17 November 2004; accepted 23 February 2005

Available online 16 June 2005

Abstract

Responses of non-uniform panels, like equipment panels of spacecraft, are not presently estimated using Statistical Energy Analysis. It is demonstrated that by treating the equipment as separate subsystems, with appropriate coupling loss factors for their connectivity, the response levels of the equipment can be estimated. The coupling loss factors are determined by the wave attenuation caused by the changes in structural properties introduced by the equipment. The estimated responses are valid at locations away from the boundary, in this case interface of the equipment. Information on the vibration levels at the interface of the equipment is necessary, especially to arrive at the random vibration loads of the equipment. A technique is developed to predict the vibration levels at locations at any distance from the interface of the equipment and validated by experiments. The prediction model is based on the interference pattern of the bending waves due to the reflection at the boundaries. It is seen that the existing techniques are suitable in estimating the responses of equipment only if the equipment behaves like mass attached at a point. But the technique developed in this study predicts the responses of the equipment that have large interface area.

© 2005 Elsevier Ltd. All rights reserved.

1. Introduction

Responses of multi-modal systems at high frequencies are normally estimated using Statistical Energy Analysis (SEA) developed by Lyon [1] and others. In SEA, the entire system is considered

*Corresponding author.

E-mail address: renji@isac.ernet.in (K. Renji).

to be an assembly of a number of structural elements, called subsystems. Solution of the equations stating the power balance of these subsystems yields the energies of the subsystems. Other response variables are derived from the known energy values. In SEA the responses are not obtained at a particular frequency but averaged over a frequency band having several modes and the response predicted is the average over an ensemble of systems. Responses at different locations are treated as ensemble of random processes and the statistical quantities like mean (spatial), variance etc., are determined.

The spatial average value of the acceleration response of the subsystem can be directly determined from the energy and the mass of the subsystem. At locations away from the boundaries, the responses at higher frequencies are not much different from the spatial average values. At such locations the spatial average value itself can give significant information. Near the boundaries the response levels are influenced by the boundary conditions and they deviate significantly from the spatially averaged responses. For simple boundary conditions the responses at the boundaries can be determined from the spatial average value. For example, at the free end of a beam the mean square response is four times the spatial average response [2].

The results discussed above are applicable for elements like solar panels and antenna reflectors of spacecraft that are having uniform structural properties. The panels/platforms of spacecraft that carry electronic equipment have highly non-uniform structural properties, especially the mass distribution. Estimation of the responses of such panels is necessary for their design as well as to arrive at the random vibration loads on the equipment for their design/testing.

There are not many studies carried out on the response of the equipment panels in SEA framework. Two studies reported in this direction are by Clarkson et al. [3] and by Kubota et al. [4]. Both the studies are applicable only when the equipment can be considered as a point mass and the panel contains only a very few equipment. In many practical situations, the equipment has a considerable interface area with the equipment and therefore cannot be treated as a point mass and the panel has a large number of equipment. As mentioned earlier the response predicted using SEA is the spatial average and is applicable only at locations away from the boundaries/interfaces. To arrive at the random vibration loads of the equipment, it is necessary to have the information on the vibration levels at the interface of the equipment. Improved technique for the prediction of the response of equipment panels is thus necessary.

In this study the response behaviour of panels with equipment attached is investigated. An analytical technique is developed to predict the vibration levels at locations at any distance from the interface of the equipment. The results are validated by experiments. They are also compared with the response estimated using the existing prediction techniques.

2. Responses of the equipment

A structurally simulated dummy of a typical electronic equipment is mounted on a panel, called equipment panel. The equipment panel without the equipment is referred here as unloaded panel.

The equipment panel considered is a honeycomb sandwich panel having dimensions 1.3×1.1 m. The face sheets are made of aluminium alloy (AL 2024) having thickness 0.19 mm each. The honeycomb core has a density of 26 kg/m^3 and the thickness of the core is 25.4 mm. Measured mass of the panel is 4.3 kg. This includes some local doublers/inserts. To calculate

modal densities, uniform mass characteristics only to be considered and the local/concentrated masses should not be considered [5]. Hence to determine the mass for modal density evaluation these concentrated mass values are subtracted from the measured mass of the panel. The value of the mass thus obtained for the calculation of the modal density is 2.75 kg. The modal density of the panel is estimated to be about 0.015/Hz at 315 Hz and 0.031/Hz at 4000 Hz [5,6]. The dissipation loss factor of the panel η_d , at frequency f is obtained in an earlier study as [7]

$$\begin{aligned} \text{for } f \leq 1250 \text{ Hz, } \eta_d &= 0.05, \\ \text{for } f > 1250 \text{ Hz, } \eta_d &= 0.02. \end{aligned} \quad (1)$$

To estimate the response to acoustic excitation, the coupling loss factors between the panel and the acoustic field have to be determined. These coupling loss factors are characterized by the parameter critical frequency of the panel [1]. The critical frequency of this panel is estimated to be 382 Hz. For this, the speed of the sound in air is assumed to be 346 m/s.

The equipment (Fig. 1) has a mass of 5.7 kg and interface dimensions 211×211 mm. It has a 5.8 mm thick base plate made of aluminium alloy having four interface holes having diameter 4.5 mm. The height of the equipment is 160.8 mm including the base plate. The panel has four M4 inserts and the equipment is attached to the panel through these inserts using allen bolts. The base plate of the equipment is in flush with the panel. The equipment used is a structural simulation of an electronic equipment used in spacecraft simulating the interface stiffness, mass and the moments of inertia. The inside portion of the equipment is hollow but a few plates are attached to simulate the required mass and moments of inertia. Fig. 2 gives a view of the equipment attached to the panel. Relative positions of the equipment and the panel can be seen in Figs. 2 and 3.

2.1. Responses of the unloaded panel

As the first step the responses of the unloaded panel, panel without the equipment, are determined. This is carried out in an earlier study [7]. The honeycomb sandwich panel is subjected to acoustic excitation in a reverberation chamber. The panel is suspended in the chamber and all the four edges of the panel are free. The sound pressure level (SPL) is measured at three locations and the acceleration responses are measured at 11 randomly selected locations on the panel. The modal overlap of this panel at 315 Hz is about 0.25. For the applicability of SEA, it is enough if one of the subsystems in energy exchange has large number of modes [7]. The response of the panel is estimated using SEA. The spatial average of the measured acceleration responses of the unloaded panel is given in Table 1 [7]. The results show a reasonably good match between the

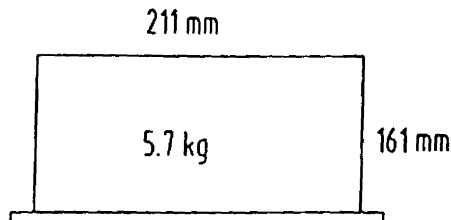


Fig. 1. Details of the equipment.



Fig. 2. Setup for the acoustic test on the panel with equipment.

predicted and measured spatial average of the acceleration response [7]. This SEA model is further used to predict the response behaviour of the panel when the equipment is attached.

The values of SPL given in Table 1 correspond to the acoustic field during the test on the panel with the equipment. The SPL values during the test on the unloaded panel are marginally different from these values. Between 500 and 2500 Hz the spatial average values of SPL during the two tests are within ± 0.1 dB and in 315 and 400 Hz they are within ± 0.5 dB.

2.2. Theoretical model for the panel with equipment

The equipment is mounted on the panel and the response of this system subjected to diffuse acoustic field is estimated using SEA.

In the SEA model the acoustic field is considered as one subsystem. The portion of the panel where the equipment is not mounted is considered to be another subsystem referred here as 'panel'. The equipment and the portion of the panel on which it is mounted is considered as another subsystem referred here as 'equipment'. Hence, the honeycomb sandwich panel having dimensions 211×211 mm together with the equipment form the subsystem 'equipment'.

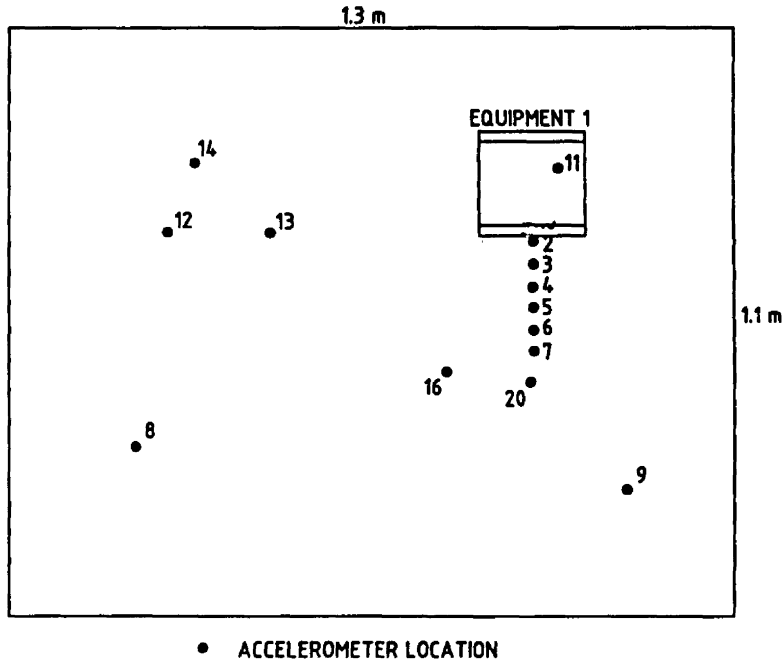


Fig. 3. Accelerometer locations.

Table 1
Acceleration response of ‘equipment’

$\frac{1}{3}$ Octave band centre frequency (Hz)	SPL (dB)	Response of the unloaded panel by experiment (g)	Response of ‘panel’ (g)		Response of ‘equipment’ (g)	
			Theory	Experiment	Theory	Experiment
315	122.8	3.9	3.7	4.3	0.51	0.47
400	126.0	6.6	7.0	5.9	0.95	0.67
500	122.7	4.7	5.7	4.5	0.73	0.58
630	118.2	3.2	3.4	2.6	0.47	0.31
800	112.3	1.5	1.7	1.5	0.26	0.20
1000	112.5	1.6	1.6	1.6	0.26	0.17
1250	113.4	1.9	1.7	1.7	0.28	0.17
1600	112.7	1.8	1.9	1.8	0.32	0.16
2000	111.9	1.9	1.7	1.8	0.29	0.19
2500	110.8	1.9	1.4	1.8	0.24	0.18

Structurally the subsystem ‘equipment’ is a rectangular plate having dimensions 211×211 mm. The flexural rigidity of this plate is the flexural rigidity of the honeycomb sandwich panel and the base plate of the equipment. Mass of this plate is 5.8 kg (equipment mass of 5.7 kg and the honeycomb sandwich panel mass of 0.1 kg). The two subsystems are coupled through a line

junction of length 0.844 (0.211 × 4) m. It is to be noted that the interface between these two subsystems is not an area junction since the portion of the panel to which the equipment is attached also is a part of the subsystem ‘equipment’. In the present analysis the reverberant acoustic field is considered as subsystem 1, ‘panel’ as subsystem 2 and ‘equipment’ as subsystem 3.

It is appropriate in SEA to consider these two subsystems as defined here since there is a large impedance difference at the line junction.

The modal density of the acoustic field is estimated using the expression given in Ref. [1] and those of ‘panel’ and ‘equipment’ are estimated using the expressions given in Refs. [5,6]. The dissipation loss factor of the unloaded panel is obtained experimentally [7] and they are given by Eq. (1). These values are used as the dissipation loss factor values for the subsystem ‘panel’ since there is no significant structural change in subsystem ‘panel’ from the unloaded panel. Not much information is available on the dissipation loss factors of equipment. Based on the suggestion by Eaton [8] on the dissipation loss factor of equipment panels, a dissipation loss factor value of 0.05 is used for subsystem ‘equipment’.

There are mainly two types of coupling paths. One coupling path is related to the structure and acoustic field. The coupling loss factors for these paths are determined by the radiation resistance characteristics. The radiation resistance of the unloaded panel [9] is considered to be the radiation resistance of the subsystem ‘panel’ as the difference between the two is very much insignificant. Radiation resistance of the ‘equipment’ is estimated theoretically. In this case the ‘equipment’ is considered to be kept on a baffle and hence the short circuiting effects on the radiation resistance can be neglected. The critical frequency of the subsystem ‘equipment’ is estimated to be very high and hence the radiation resistance is expected to be very low. Hence these approximations are not expected to make significant effects on the estimated responses.

The other important power flow path is between the ‘panel’ and the ‘equipment’. The coupling loss factor for this power flow is determined by the wave attenuation at the interfaces of the two subsystems. The wave attenuation in the present case is caused due to the change in mass/moment of inertia and flexural rigidity which are introduced by the equipment. The coupling loss factor for this power flow is given by

$$\eta_{23} = 2c_{b,2}L\tau_{23}/(\pi\omega A_2), \quad (2)$$

where $c_{b,2}$ is the speed of the bending wave in subsystem 2 and A_2 is the area of subsystem 2. In Eq. (2), L is the length of the line junction and τ_{23} is the wave transmission coefficient. The wave transmission coefficient is obtained from the analysis of wave attenuation due to the change in structural properties. Cremer, Heckl and Ungar [10] have made several studies on this behaviour for different types of waves. They have shown that for bending waves

$$\tau_{23} = [2\sqrt{\kappa\chi}(1 + \kappa)(1 + \chi)/\{\kappa(1 + \chi)^2 + 2\chi(1 + \kappa^2)\}]^2. \quad (3)$$

The parameter κ is the ratio of the speeds of the bending waves,

$$\kappa = c_{b2}/c_{b3}, \quad (4)$$

and the parameter χ is given by

$$\chi = (c_{b,2}^2/D_2)/(c_{b,3}^2/D_3). \quad (5)$$

As discussed the coupling between ‘panel’ and the ‘equipment’ is due to the attenuation of the bending waves at the junction. This coupling is expected to be weak as there is a large difference in the impedance of the bending waves. For example, the impedance of the bending waves in the subsystem ‘panel’ is about 600 kg/m s and that in the subsystem ‘equipment’ is about 19000 kg/m s at 315 Hz.

Having obtained the values of the radiation resistance, structural coupling loss factors and the dissipation loss factors, the response of the system is estimated using SEA. Acceleration responses of the panel and the equipment thus estimated are given in Figs. 4 and 5 and in Table 1.

2.3. Experimental results for the panel with equipment

The equipment is mounted on the honeycomb panel and subjected to diffuse acoustic loads in a reverberation chamber. The test setup is shown in Fig. 2. The excitation SPL is given in Table 1. The vibration levels are measured at several locations which are shown in Fig. 3. It is important that the locations used for spatial average are away from the boundary of the subsystems. In the present case, the line interface between the panel and the equipment also is a boundary of the subsystems and hence the measurement locations used for the spatial average are away from this line interface. Acceleration levels of the panel are measured at seven locations namely 8, 9, 12, 13, 14, 16 and 20. Response of the equipment is measured at location 11. Location 11 is actually on the panel but on the rear side and away from the interface of the equipment with the panel. The spatial average values of the measured acceleration responses of the panel and the equipment are obtained in 1/3 octave bands and given from 315 to 2500 Hz in Table 1, Figs. 4 and 5.

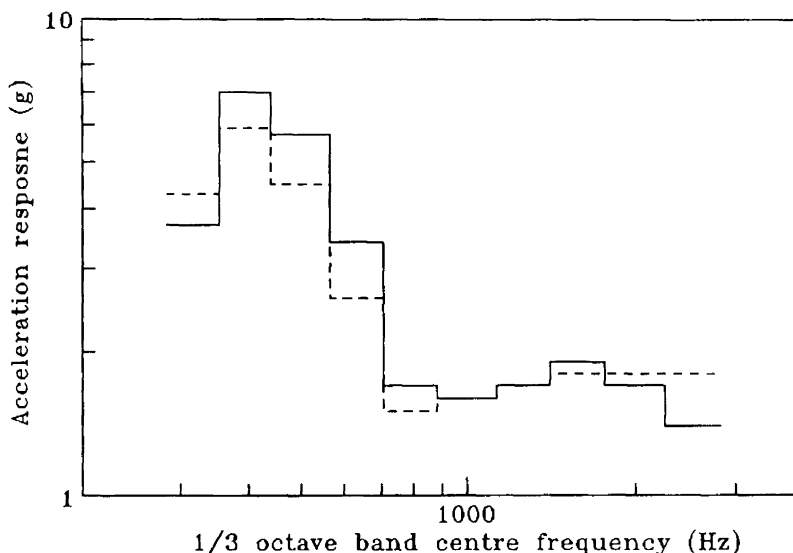


Fig. 4. Response of the panel when equipment is mounted: —, theory; - - -, experiment.

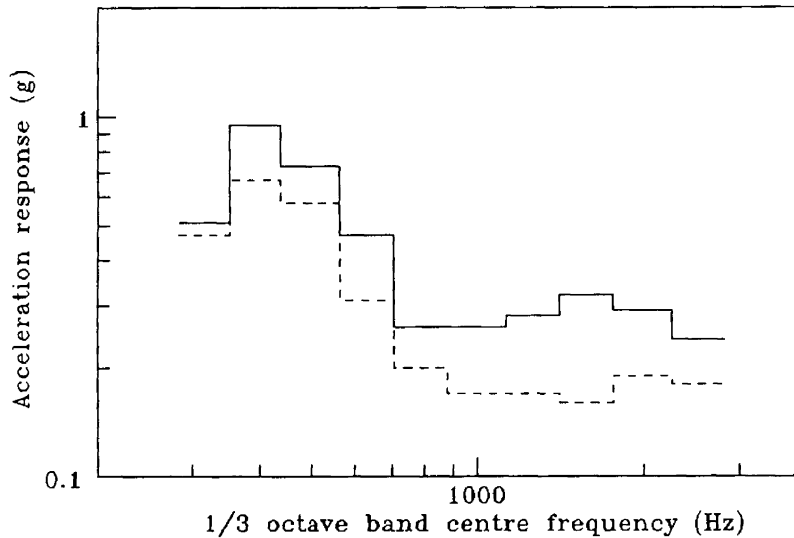


Fig. 5. Response of the equipment: —, theory; - - -, experiment.

2.4. Discussion of results

The estimated spatial average values of the acceleration responses match reasonably well with the experimental results. Thus, the response of the equipment can be estimated in SEA framework by treating it as a separate subsystem with appropriate coupling loss factors. It is to be noted that the predicted response of the equipment is the spatial average of the responses at locations on the subsystem ‘equipment’ away from the interface junction.

It can be observed from the results given in Table 1 that the spatial average values of the acceleration responses of the panel are practically unchanged due to the introduction of the equipment. This is because only one equipment is mounted on the panel. If several equipment are mounted, the response of the ‘panel’ is expected to be lower than that of the unloaded panel.

It is interesting to study the estimated acceleration response of the equipment if the structural path is neglected in the analysis. This means that $\eta_{23} = \eta_{32} = 0$. The estimated results are given in Table 2. The results show that the response of the equipment is mainly from the response of the panel through the structural coupling. The response due to direct acoustic excitation is negligible and the response is mainly from the structural path.

Thus, it is seen that by treating the equipment and the portion of the panel on which the equipment is mounted as a separate subsystem, the response level of the equipment can be estimated in SEA formulation. In this model, a line junction exists between the ‘panel’ and the ‘equipment’. The coupling loss factors between the panel and the equipment can be obtained from the characteristics of the bending wave attenuation caused due to change in structural properties. The estimated response of the equipment is valid only at locations away from the line junction. The significant part of the response of the equipment is from the response of the panel and the vibration due to direct acoustic excitation is negligible.

Table 2
Response of the 'equipment' with and without the structural path

$\frac{1}{3}$ Octave band centre frequency (Hz)	Acceleration response (g)	
	With structural path	Without structural path
315	0.51	0.035
400	0.95	0.049
500	0.73	0.031
630	0.47	0.016
800	0.26	0.0073
1000	0.26	0.0062
1250	0.28	0.0056
1600	0.32	0.0040
2000	0.29	0.0029
2500	0.24	0.0019

3. Responses close to interface of equipment

It is demonstrated previously that the dynamic response of equipment can be estimated by treating it as a separate subsystem in the SEA model. It is also stated that the response levels thus obtained are valid only at locations far away from the boundary, in this case the interface of the equipment with the panel. In arriving at the random vibration specifications for the equipment, it is necessary to have the information on the response levels at these boundaries. In many practical situations it will not be possible to measure the responses at the interface of the equipment with the panel but the acceleration levels are measured on the panel at a distance from the interface with the equipment. In such cases, it is necessary to have the relation between the measured vibration levels and the acceleration levels at the boundaries. Thus, it is essential to be able to predict the response levels at a given distance from the interface of the equipment with the panel. SEA does not predict the response at the boundaries which is a major limitation of SEA. In this study a prediction technique is developed by which this could be achieved. In this model the response at any location is obtained from the knowledge of the interference pattern of the bending waves. The model is validated by the experimental results.

3.1. Experimental results

Response levels at specific distances from the interface of the equipment are measured. Vibration levels are measured during the same test which was carried out for measuring the vibration level of the equipment. Hence, the test setup is the same as given by Fig. 2. Locations at which acceleration levels are measured are shown in Fig. 3. Location 2 is on the panel close to the centre of the edge of the equipment. Location 10 is similar to the location 2 but on the base plate of the equipment. Locations 3–7 are on the panel at specific distances from the equipment. Location 3 is at a distance of 20 mm, location 4 is at a distance of 40 mm and location 5 is at a distance of 60 mm from location 2. The distance of location 6 is 90 mm and that of location 7 is

120 mm from location 2. The diameter of the accelerometer is about 7 mm and the distances mentioned are the values up to the centre of the accelerometers.

The excitation SPL during the test is as given in Table 1. The vibration levels measured at the above locations are given in Table 3. The spatial average of the measured acceleration levels, which is obtained from seven locations namely 8, 9, 12, 13, 14, 16 and 20, is also given in the same table which is the same as the one given in Table 1.

The results show some interesting behaviour. Consider the variation of the response with the distance from the equipment interface that is from location 2 to 7. The vibration levels are different depending on the distance of the measurement location from the interface of the equipment with the panel. The response levels gradually increase with the distance from the equipment interface and converge to the spatial average value of the responses of the panel. For a better understanding the responses at 315, 800, 1250 and 2000 Hz are plotted against the distance from the equipment interface in Figs. 6–9. The responses of the ‘panel’ are also shown in the same figures at the end of the curve. The results show that the responses converge to the responses of the panel at some distance from the interface of the equipment and this distance is lesser at higher frequencies.

It can be seen that the responses converge to the spatial average by about a distance of $\lambda_b/4$ from the boundary where λ_b is the wavelength of the bending wave in the panel. For example consider location 7 which is at a distance of 125 mm from the boundary. One can observe that the

Table 3
Acceleration response at a distance from equipment

Freq. (Hz)	Acceleration response (g)						
	2	3	4	5	6	7	‘Panel’
315	0.89 (1.7)	1.2 (2.0)	1.4 (2.2)	1.6 (2.5)	2.1 (2.9)	2.6 (3.3)	4.3
400	2.7 (3.2)	3.3 (3.7)	3.4 (4.2)	3.9 (4.7)	4.3 (5.5)	4.9 (6.2)	5.9
500	3.4 (3.4)	3.7 (3.8)	4.1 (4.2)	4.5 (4.5)	4.9 (5.1)	5.1 (5.7)	4.5
630	1.5 (2.0)	1.5 (2.2)	1.6 (2.5)	1.8 (2.7)	1.9 (3.2)	2.0 (3.7)	2.6
800	0.46 (0.83)	0.59 (0.96)	0.69 (1.1)	0.87 (1.3)	1.0 (1.6)	1.2 (1.9)	1.5
1000	0.59 (0.71)	0.78 (0.84)	0.89 (1.0)	1.2 (1.2)	1.3 (1.6)	1.5 (1.9)	1.6
1250	0.77 (0.66)	1.1 (0.81)	1.1 (1.0)	1.4 (1.3)	1.5 (1.8)	1.5 (1.8)	1.7
1600	0.90 (0.69)	1.2 (0.85)	1.3 (1.1)	1.6 (1.5)	1.9 (2.1)	1.9 (2.0)	1.8
2000	0.99 (0.53)	1.3 (0.71)	1.4 (1.1)	1.6 (1.5)	1.8 (1.7)	1.7 (1.8)	1.8
2500	0.86 (0.38)	1.2 (0.57)	1.2 (0.96)	1.4 (1.4)	1.6 (1.4)	1.4 (1.5)	1.8

Note: The values given in brackets are theoretically estimated.

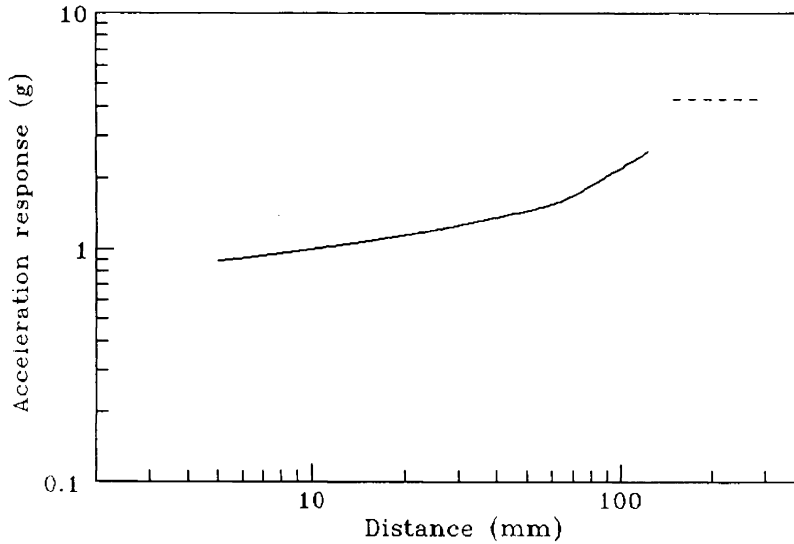


Fig. 6. —, Variation of response with distance from the equipment at 315 Hz; - - -, response of the panel.

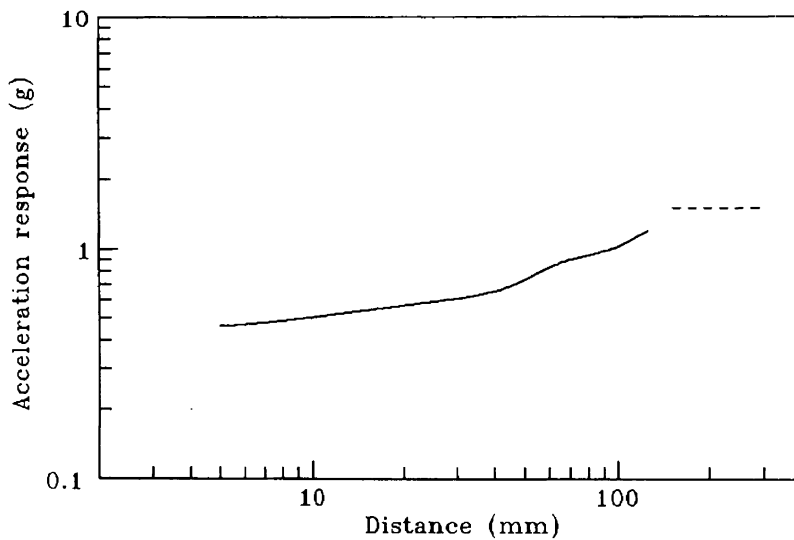


Fig. 7. —, Variation of response with distance from the equipment at 800 Hz; - - -, response of the panel.

response at location 7 is close to the panel response beyond 1000 Hz. The expected wavelength of the bending wave at 1000 Hz is about 0.54 m.

The response of the equipment represented by location 11 is entirely different from the response at the interface of the equipment with the panel, that is the response at location 2. The response of the equipment predicted by SEA is not valid at locations near to the interface and clearly a different technique is necessary to predict the vibration levels at these locations.

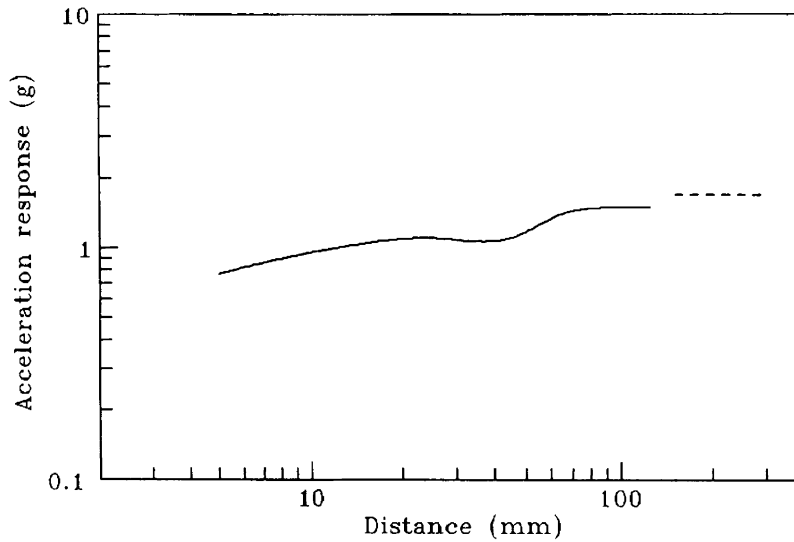


Fig. 8. —, Variation of response with distance from the equipment at 1250 Hz; - - -, response of the panel.

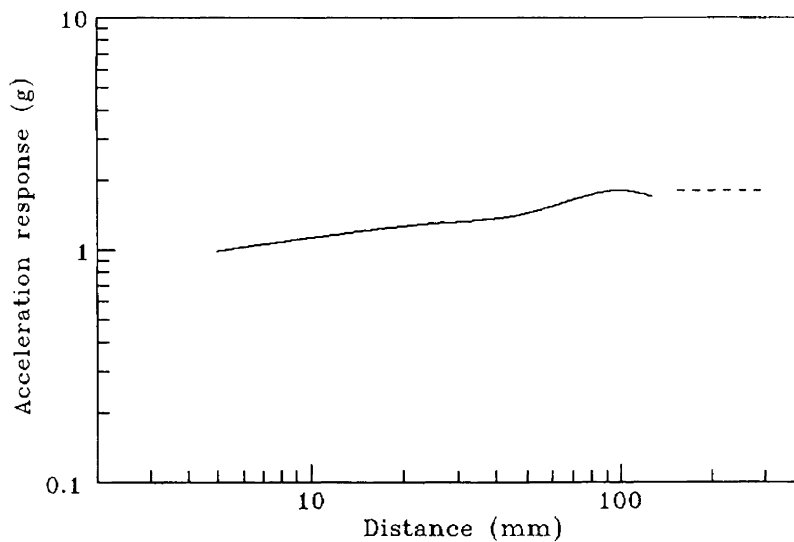


Fig. 9. —, Variation of response with distance from the equipment at 2000 Hz; - - -, response of the panel.

3.2. Theoretical estimates

Consider a bending wave traveling in the x -direction. When this wave reaches the boundary, which is the line interface of the equipment with the panel, it undergoes reflection. The reflected wave will have, in general, a near-field component and a far-field component. The near-field component reduces with the distance from the boundary. Let B be the amplitude of the velocity of the incident wave. The far-field component of the reflected wave has an amplitude of C and the

amplitude of the near-field component at the junction is D . In general, C and D are complex numbers. The velocity of the resultant wave field is then given by

$$v = B e^{j(\omega t - kx)} + C e^{j(\omega t + kx)} + D e^{kx} e^{j\omega t}, \tag{6}$$

which can be simplified as

$$v = \{B e^{-jkx} + C e^{jkx} + D e^{kx}\} e^{j\omega t}. \tag{7}$$

Defining, $r_n = C/B$ and $r_f = D/B$, the velocity field is given by

$$v = B \{e^{-jkx} + r_n e^{jkx} + r_f e^{kx}\} e^{j\omega t}. \tag{8}$$

The parameters r_n and r_f are, in general, complex numbers. Let

$$r_n = G + jH \quad \text{and} \quad r_f = P + jQ. \tag{9}$$

Substituting Eq. (9) in Eq. (8) we get

$$v = B [\{\cos(kx) + G \cos(kx) - H \sin(kx) + P e^{kx}\} - j \{\sin(kx) - G \sin(kx) - H \cos(kx) - Q e^{kx}\}] e^{j\omega t}. \tag{10}$$

The mean square value of the velocity at any point is given by

$$\langle v^2 \rangle_t = (B^2/2) [\{(1 + G) \cos(kx) - H \sin(kx) + P e^{kx}\}^2 + \{(1 - G) \sin(kx) - H \cos(kx) - Q e^{kx}\}^2]. \tag{11}$$

At locations far away from the boundary, the vibration field is diffused. The spatial average value of this diffuse field can be obtained by taking the spatial average of Eq. (11) after removing the near field terms which vanish at locations far away from the boundary.

$$\langle v^2 \rangle_x = (B^2/2) [\{(1 + G)^2 \langle \cos^2(kx) \rangle_x + H^2 \langle \sin^2(kx) \rangle_x + (1 - G)^2 \langle \sin^2(kx) \rangle_x + H^2 \langle \cos^2(kx) \rangle_x - 4H \langle \sin(kx) \cos(kx) \rangle_x \}. \tag{12}$$

It can be shown that

$$\langle \sin(kx) \cos(kx) \rangle_x = 0, \quad \langle \sin^2(kx) \rangle_x = 0.5 \quad \text{and} \quad \langle \cos^2(kx) \rangle_x = 0.5. \tag{13}$$

Using the relations given by Eq. (13) in Eq. (12) and upon simplification, the equation for the spatial average of the velocity becomes

$$\langle v^2 \rangle_x = (B^2/2) \{1 + G^2 + H^2\}. \tag{14}$$

From the above equation for the spatial average of the velocity, an expression for B^2 can be obtained as

$$B^2 = 2 \langle v^2 \rangle_x / \{1 + G^2 + H^2\}. \tag{15}$$

The spatial average value of the velocity away from the boundary can be predicted by SEA. Hence, the term $\langle v^2 \rangle_x$ in Eq. (15) can be determined using SEA. For the known values of transmission coefficient, that is G and H , the value of B^2 can now be obtained using Eq. (15). Once the value of B^2 is determined, the mean square value of the velocity at any location can be estimated using Eq. (11).

The values of the parameters r_n and r_f for the bending waves are derived by Cremer et al. [10]. For the case where the wave reflection is due to change in structural properties the above parameters are given by

$$r_n = \{2\chi(1 - \kappa^2) - j\kappa(1 - \chi)^2\} / \{\kappa(1 + \chi)^2 + 2\chi(1 + \kappa^2)\}, \quad (16)$$

$$r_f = \{\kappa(1 - \chi^2) - j\kappa(1 - \chi)^2\} / \{\kappa(1 + \chi)^2 + 2\chi(1 + \kappa^2)\}. \quad (17)$$

The parameters κ and χ are given by Eqs. (4) and (5). The experimental results clearly showed that the response levels converged to the SEA result by a distance of $\lambda_b/4$ from the boundary. Hence, the response levels at locations, which are away from the boundary by a distance more than $\lambda_b/4$, are given by SEA. At locations which are within $\lambda_b/4$ distance from the boundary, the vibration levels can be estimated using the SEA result in conjunction with Eqs. (11), (14), (16) and (17).

Using this technique the response levels at various locations close to the equipment are estimated and are given in brackets in Table 3. The estimated results show a similar trend as shown by the measured values, that is increase in response with the distance from the equipment interface. In Table 3, the estimated response levels are compared with the measured vibration levels. The results can be compared in Figs. 10–13 for locations 2, 3, 5 and 7. The estimated results are reasonably in good agreement with the measured vibration levels. The results also show that further improvement in the prediction technique is necessary. One possible improvement is the use of refined coupling loss factors for panel and equipment junctions. It is also to be noted that in the present analysis the equipment is considered as mass/moment of inertia applied uniformly over the equipment interface area considering the stiffness at the interface. The modes are due to the local stiffness of the mounting platform (the panel) along with the interface stiffness of the equipment and the mass/moment of inertia of the equipment. The technique could be further improved by incorporating the natural modes of the equipment.

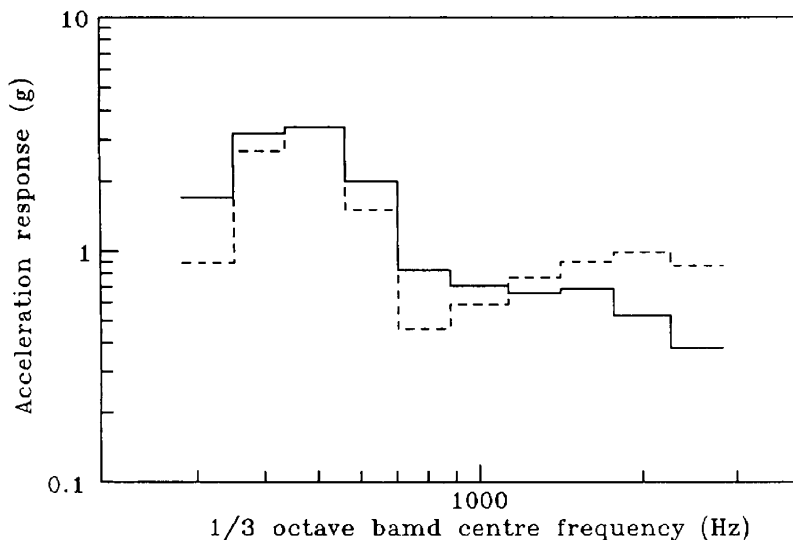


Fig. 10. Response at location 2: —, theory; - - -, experiment.

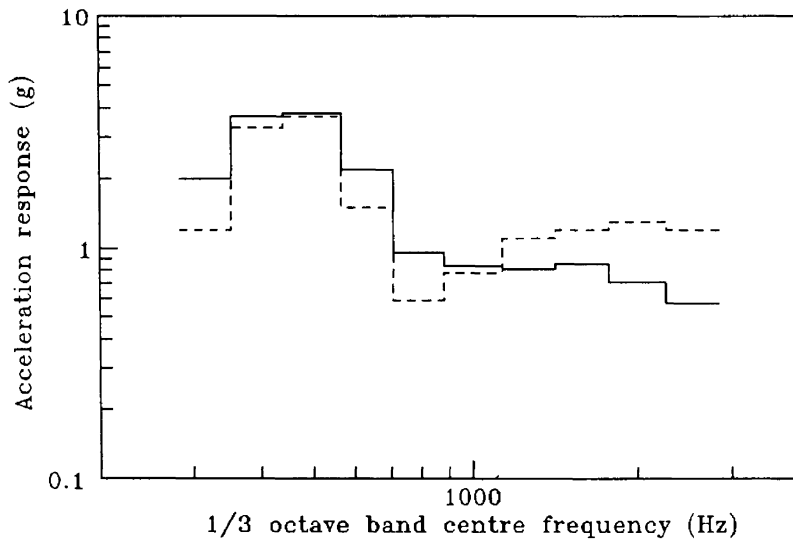


Fig. 11. Response at location 3: —, theory; - - -, experiment.

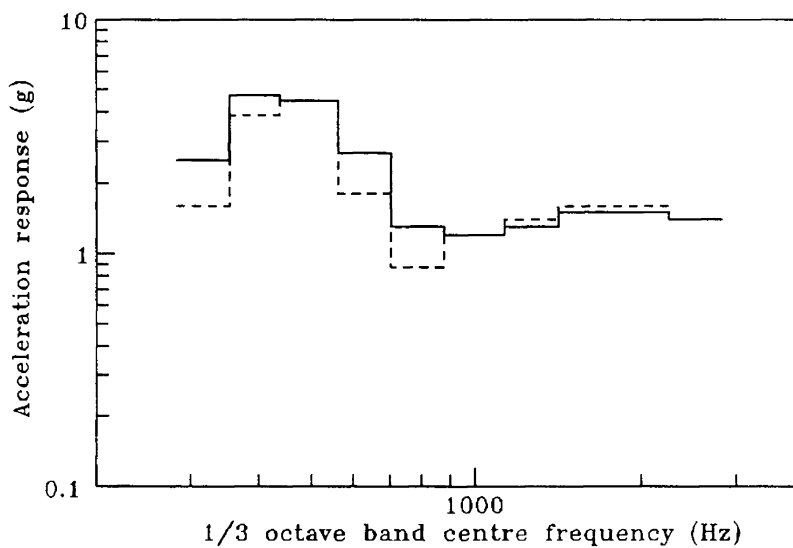


Fig. 12. Response at location 5: —, theory; - - -, experiment.

4. Comparison with the existing techniques

It is now interesting to compare the measured vibration levels with those results estimated using the existing techniques. There are mainly two methods existing for response estimation of equipment panels, one based on the change in the admittance of the panel due to the addition of the equipment and the other based on Asymptotic Modal Analysis (AMA) results.

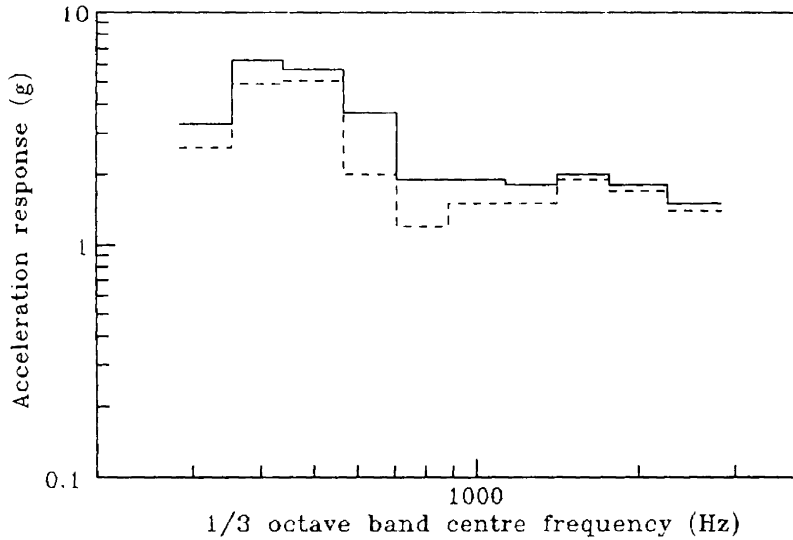


Fig. 13. Response at location 7: —, theory; - - -, experiment.

4.1. Point impedance model

This technique is developed by Clarkson et al. [2]. Let Z_p be the average driving point impedance of the unloaded panel and $\langle a_p^2 \rangle_x$ be the mean square value of the acceleration response. In this model, it is assumed that the equipment is attached at a point on the panel. Due to the attachment of the equipment, the impedance at the attachment point is now different from Z_p . The response of the equipment is estimated based on the difference in the impedance values. If the impedance of the equipment is Z_b , the impedance of the panel at the equipment attachment point is considered to be $Z_p + Z_b$. Clarkson et al. [2] showed that the acceleration response of the equipment $\langle a_b^2 \rangle_x$ is related to the response of the bare panel by the equation

$$\langle a_b^2 \rangle_x = \langle a_p^2 \rangle_x \{ |Z_p|^2 / |Z_p + Z_b|^2 \}. \quad (18)$$

The impedance of the equipment can be approximated by the equation

$$Z_b = j\omega M, \quad (19)$$

where M is the mass of the equipment. It is to be noted that the impedance referred here is the impedance of the mass. Whereas the impedance mentioned previously (Section 2.2) is the impedance of the bending waves. Clarkson et al. [3] have suggested the use of total mass of the equipment divided by the number of attachment points as the mass required for calculating the impedance using Eq. (19). As further improvement they used measured impedance values. Measured impedance values follow Eq. (19), at low frequencies. At higher frequencies the measured impedance is generally lower than that given by Eq. (19) due to presence resonance.

The impedance of the panel can be obtained from experiments. However, the impedance can be estimated in the following way. For a thin plate the average driving point impedance is

given by [1]

$$Z_p = 8(\rho D)^{0.5}. \quad (20)$$

In general, the real part of the admittance can be obtained from the modal density using the relation [11]

$$\langle \text{Re}(Y) \rangle = n(f)/4M, \quad (21)$$

where M is the mass of the panel. If it is assumed that the imaginary part of the admittance is negligible, one can use the above equation to estimate the impedance of the unloaded panel. For a thin plate, that is if shear effects are negligible, the imaginary part of the impedance is zero.

The impedance of the equipment is measured by exciting the equipment alone and found that Eq. (19) can be used to obtain the impedance up to 1400 Hz. Hence, the response is estimated with the impedance of the equipment given by Eq. (19) without causing any significant error in the estimation. The impedance of the panel is estimated using Eq. (20) and use of this expression in this case will not make any significant error in the estimated impedance. This is because the transverse shear effects are not that significant and hence the imaginary part of the impedance can be neglected. For example the modal density of the unloaded panel estimated without considering the transverse shear effects is about 0.014. The modal density estimated incorporating the transverse shear effects is about 0.017 at 1000 Hz. However, the impedance is calculated using the estimated modal density incorporating the transverse shear effects.

The estimated and the measured results are given in Table 4. The estimated responses are compared with the acceleration levels measured at location 2. The point impedance model predicts the response based on the change in the impedance and the impedance change occurs at the interface of the equipment. Hence the responses predicted by point impedance model are compared with the results measured at the interface of the equipment (location 2). It can be observed that the existing technique grossly underestimates the response. A reasonable match is seen only at low frequencies, that too only at 315 Hz. The existing technique is suitable for equipment having small interface area. But the technique developed in this study predicts the responses that are reasonably matching with the measured vibration levels.

Table 4
Response using point impedance model

$\frac{1}{3}$ Octave band centre frequency (Hz)	Acceleration response (g)	
	Theory	Measured at loc. 2
315	0.66	0.89
400	0.95	2.7
500	0.56	3.4
630	0.28	1.5
800	0.12	0.46
1000	0.089	0.59
1250	0.072	0.77
1600	0.060	0.90
2000	0.041	0.99
2500	0.025	0.86

4.2. AMA Model

Kubota et al. [4] developed a model to estimate the response of the equipment attached to a plate using asymptotic modal analysis. Using this technique

$$\langle a_b^2 \rangle_x = \langle a_p^2 \rangle_x \{ (2\lambda_b^2 \rho / \pi^2 M)^2 / [1 + (2\lambda_b^2 \rho / \pi^2 M)^2] \}, \quad (22)$$

where λ_b is the wavelength in the plate. The estimated response levels are given in Table 5. In this case it is more appropriate to compare the estimated response with the response of the equipment, that is location 11, since the AMA model predicts the response of the concentrated mass.

The results show that the estimated response is in agreement with the measured results at low frequencies. At higher frequencies the predicted response is very low. The AMA model is accurate in predicting the response if the dimension of the equipment is very small, that is the dimension is far less than $\lambda_b/4$. But it does not predict the response at the interface. The technique developed in this study predicts the response of the equipment as well as the response at the interface.

5. Conclusions

It is shown that the response of an equipment mounted on a panel can be estimated using SEA. This is done by treating the portion of the panel on which the equipment is not mounted as one subsystem and the portion of the panel on which the equipment is mounted together with the equipment as another subsystem. The coupling loss factor for the line junction between these two subsystems is caused by the wave attenuation due to changes in structural properties. Measured responses of a honeycomb sandwich panel mounted with equipment, subjected to diffuse acoustic field, agree reasonably well with the responses estimated using this SEA model.

The vibration levels at locations away from the equipment are significantly larger depending on the distance from the equipment. The experimental results showed that the SEA result is valid only beyond a distance of $\frac{1}{4}$ of the wavelength in the subsystem. An analytical technique, which is

Table 5
Response using AMA model

$\frac{1}{3}$ Octave band centre frequency (Hz)	Acceleration response (g)	
	Theory	Measured at loc. 11
315	0.41	0.47
400	0.50	0.67
500	0.33	0.58
630	0.16	0.31
800	0.060	0.20
1000	0.046	0.17
1250	0.038	0.17
1600	0.033	0.16
2000	0.022	0.19
2500	0.014	0.18

based on the interference pattern of the bending waves due to reflection at the boundaries, is developed to predict the response at any distance from the boundary. Responses estimated at various locations using this technique match reasonably well with the measured results.

The measured vibration levels are also compared with the results estimated using the existing techniques such as point impedance model and AMA. It is seen that both the models significantly under-estimate the response levels. These prediction models are suitable in estimating the response of point masses but not adequate for predicting the response of the equipment of spacecraft that have large interface area as considered in the present investigation. The prediction technique developed in this study significantly improves the prediction.

Acknowledgement

Authors wish to thank Mr. K.N. ArunKumar, Mr. K.R. Chandrasekhar, Mr. S. Murugan and Ms. D. Padmini of Acoustic Test Facility, National Aerospace Laboratories, Bangalore, India, for their valuable help in conducting the experimental work.

Appendix A. List of symbols

Symbols not listed here are used only at specific places and are explained wherever they occur. Single and double over-dots represent first and second derivatives with respect to time. Since the process considered are stationary random, the dynamic variables discussed are the long time averaged quantities and in such cases the notation for the averaging is dropped. For example $\langle a^2 \rangle_t$ is written as a^2 .

A	area of plate
a	acceleration response of a structure
a_p	acceleration response of a plate
a_b	acceleration response of an equipment
c_{bi}	velocity of the bending wave in subsystem i
D_i	flexural rigidity of plate i
f	frequency, in Hz
j	complex operator
k	Wavenumber
L	length of the line junction or boundary
M	mass of a structure/equipment
$n(f)$	modal density
$\text{Re}(x)$	real part of x
t	Time
Y	driving point admittance
v	velocity of a structure
Z_p	driving point impedance of a structure
Z_b	impedance of an equipment
η_d	dissipation loss factor

η_{ij}	coupling loss factor for subsystem i to j
λ_b	wavelength of the bending wave
ω	circular frequency, in rad/s
ρ	mass per unit area
τ_{ij}	wave transmission coefficient for subsystems i to j
$\langle \rangle_x$	average over the domain x
$\langle \rangle$	average over the time domain

References

- [1] R.H. Lyon, *Statistical Energy Analysis of Dynamical Systems: Theory and Applications*, MIT Press, Cambridge, MA, 1975.
- [2] R.H. Lyon, R.G. Dejong, *Theory and Application of Statistical Energy Analysis*, Butterworth-Heinemann, Newton, MA, 1995.
- [3] B.L. Clarkson, R.J. Pope, M.F. Ranky, *Study of the evolution of structural acoustic design guides*, vol. 2, ESA CR(P)-1609, 1981.
- [4] Y. Kubota, S. Sekimoto, E.H. Dowell, The high frequency response of a plate carrying a concentrated mass, *Journal of Sound and Vibration* 138 (1990) 321–333.
- [5] B.L. Clarkson, M.F. Ranky, Modal density of honeycomb plates, *Journal of Sound and Vibration* 91 (1983) 103–118.
- [6] L.L. Erickson, Modal densities of sandwich panels: Theory and experiment, *Shock and Vibration Bulletin* 39 (1969) 1–16.
- [7] K. Renji, On the number of modes required for statistical energy analysis-based calculations, *Journal of Sound and Vibration* 269 (2004) 1128–1132.
- [8] D.C.G. Eaton, *Structural acoustic design manual*, ESA PSS-03-1201, issue 1, 1987.
- [9] K. Renji, On the effect of boundaries on radiation resistance of plates, *Journal of the Acoustical Society of America* 110 (2001) 1253–1255.
- [10] L. Cremer, M. Heckl, E.E. Ungar, *Structure-borne Sound*, Springer, Berlin, 1973.
- [11] B.L. Clarkson, The derivation of modal densities from point impedances, *Journal of Sound and Vibration* 77 (1981) 583–584.